High-Pressure and High-Temperature Excess Adsorption Isotherms of N_2, CH_4, and C_3H_8 on Activated Carbon

Marc G. Frère* and Guy F. De Weireld

Faculté Polytechnique de Mons, Thermodynamics Department, 31 bd Dolez, B-7000 Mons, Belgium

This paper presents experimental excess adsorption isotherms of N_2, CH_4, and C_3H_8 on activated carbon (F30/470 from Chemviron Carbon) at five different temperatures (303 K, 323 K, 343 K, 363 K, and 383 K). The whole pressure range is covered for subcritical conditions and the maximum pressure is 10 MPa for supercritical conditions. The adsorption device is a magnetic suspension balance which has been instrumented and automated for adsorption measurements in the range of high temperatures and high pressures (303 K to 423 K, 0 to 10 MPa). The coherence of the results is checked by comparing the N_2 data at 303 K to those obtained by a classical volumetric apparatus. Discrepancies appear to be less than 3.5%. The influence of the buoyancy effect on the results is discussed.

Introduction

For the past 10 years, important research programs have been focused on emerging technologies involving gas adsorption. For example, natural gas storage by adsorption, sorption refrigerating machines and thermotransformers, adsorption of uncompletely burnt hydrocarbons from combustion gases, and natural gas recovery from coal mines are technologies of great interest. The development of such technologies requires basic adsorption data (equilibrium and kinetics) in wide ranges of experimental conditions, that is, generally high temperatures or/and high pressures. For example, considering the particular application of natural gas storage by adsorption, one must identify the best adsorbent and the most appropriate filling pressure which will lead to values of storage capacities that can be compared to the classical compressed natural gas storage. The experimental study should include the determination of adsorption isotherms at pressures up to 10 MPa. The adsorption and desorption thermal effects must also be studied as they affect the charge and discharge operations.[1−4] The same kind of experimental study including adsorption isotherms determination is also necessary for the determination of the performances of adsorption heat pumps, thermotransformers, and refrigerating machines.[5−7] The temperature and pressure conditions are set by the temperatures of the heat reservoirs and by the adsorbate properties. For example, a refrigerating machine working with ammonia as a refrigerant, producing cold at 263 K and rejecting heat at 303 K, would be characterized by low and high pressures respectively equal to 291 kPa and 1167 kPa. The maximum temperature reached by the adsorbent is the hot reservoir temperature during the desorption−condensation process (for example, 423 K); the lowest temperature of the adsorbent is the medium reservoir temperature, that is, 303 K. Considering different adsorbates and different heat reservoir temperatures would lead to extremely wide ranges of temperature and pressure conditions to be studied.

The need for adsorption data in such particular ranges of temperature and pressure appeals for specific equipment. High-pressure adsorption data remain rare in the literature,[8−10] although more and more laboratories are now aware of their importance. Simultaneous high-temperature (above 323 K) and high-pressure (above the atmospheric pressure) adsorption data are even more difficult to find: the main obstacle to the acquisition of such data is the limitation in temperature set by the electronic components (pressure and mass sensors, electrovalves) of the adsorption apparatus. Some existing apparatuses may work at high temperature but this high temperature is reached only in the vicinity of the sample; the sensors must remain at ambient temperature. Consequently, it is impossible to perform simultaneous high-temperature and high-pressure data measurements for fluids which could condense in the cold spot of the apparatus. Such special measurements require a completely thermostated installation.

An adsorption apparatus based on the gravimetric principle was developed in our laboratory to overcome these difficulties. It consists of a magnetic suspension balance which was instrumented to achieve completely automated adsorption isotherms measurements for pressures up to 10 MPa and for temperatures ranging from 303 K to 423 K. Besides, it makes possible the study of adsorbates which are liquid in ambient conditions. The experimental device is briefly presented. Details may be found elsewhere.[11,12] This paper is devoted to the presentation of experimental excess adsorption isotherms for N_2, CH_4, and C_3H_8 on activated carbon (F30/470 Chemviron Carbon) at five temperatures, namely, 303 K, 323 K, 343 K, 363 K, and 383 K. Both supercritical and subcritical data are thus provided. For N_2 at 303 K the results are compared to those obtained with a volumetric apparatus. This volumetric apparatus was previously described and has provided a large number of published data.[10,13,14] The influence of the buoyancy effect is discussed.

Experimental Section

Materials. Activated carbon (F30/470) was provided by Chemviron Carbon, Belgium. Table 1 gives its main structural characteristics (micropore volume V_{mP}, total pore volume V_P, micropore surface area A_{mP}). The gases, N_2, CH_4, and C_3H_8, are provided by L'Air Liquide Belgium with

* To whom correspondence should be addressed. E-mail: Marc.Frere@fpms.ac.be. Fax: 32/65/37 42 09.

10.1021/je010257s CCC: $22.00
Published on Web 04/27/2002

Table 1. Main Structural Characteristics of Activated Carbon F30/470 Chemviron Carbon (V_{mP}: Total Micropore Volume Obtained by the *t*-Plot Method; V_P: Total Pore Volume; A_{mP}: Specific Surface Area of the Micropores Obtained by the *t*-Plot Method)

	V_{mP}, $m^3\ kg^{-1}$	V_P, $m^3\ kg^{-1}$	A_{mP}, $m^2\ kg^{-1}$
F30/470	0.394×10^{-3}	0.497×10^{-3}	993.5×10^3

Table 2. Critical Temperature T_c and Critical Pressure P_c for N_2, CH_4, and C_3H_8[15]

adsorbate	T_c, K	P_c, kPa	adsorbate	T_c, K	T_c, kPa
N_2	126.20	3400	C_3H_8	369.80	4242
CH_4	190.55	4595			

purities of 99.996 vol %, 99.995 vol %, and 99.5 vol %, respectively. Table 2 gives the critical temperature T_c and pressure P_c for these adsorbates.[15]

Equipment. The adsorption apparatus is based on the gravimetric principle. The adsorbed mass is measured by a magnetic suspension balance. Its principle is illustrated in Figure 1.

It consists of a crucible (C) suspended to a permanent magnet (PM) by a coupling system (CS). The permanent magnet is kept in a suspension state due to the electromagnet (EM) which hangs from the hook of an analytical balance (AB). The force due to the mass uptake during the adsorption process is transmitted to the analytical balance by the magnetic suspension (coupling of the permanent magnet and electromagnet). The position of the permanent magnet is kept constant by a regulation system including a sensor core (SCR), a sensor coil (SCL) which detects the position of the permanent magnet, and a PID controller which regulates the position of the permanent magnet by changing the current circulating in the electromagnet. Given the fact that the position of the permanent magnet is constant, the force transmitted to the analytical balance is equal to the weight of the crucible−adsorbent−adsorbed phase system. The crucible, the coupling system, and the permanent magnet are located in the adsorption chamber (AC), in which the adsorbate is introduced at the experimental temperature and pressure.

This magnetic suspension balance has been instrumented to perform automated isotherms measurements at high temperature and high pressure. The rest of the installation mainly consists of pipes, electrovalves, pressure, and temperature sensors. The adsorption chamber is linked to a gas reservoir and to a vacuum pump. It is discussed in a previous paper.[12] The gas admission and evacuation steps are controlled by electrovalves. The pressure is measured by a pressure transducer operating between 0 MPa and 10 MPa. The operating range may be selected by the operator: the minimum working range is 0 MPa to 0.5 MPa. The temperature is measured by a Pt100. The adsorption chamber, the electovalves, and the sensor part of the pressure transducer and of the Pt100 are located in an incubator which ensures a constant temperature in the whole installation. It provides temperatures from ambient to 423 K. Each component of the installation in contact with the gas is at the experimental temperature whereas the electronic material is at ambient temperature. The maximum experimental temperature and/or pressure are no longer limited by the resistance of the electronic material or by the condensation of the adsorbate in the cold spots of the installation. Besides, for subcritical fluids, increasing the maximum allowable temperature increases the maximum allowable experimental pressure. The installation can operate from vacuum to 10 MPa and for temperatures ranging from 303 K to 423 K.

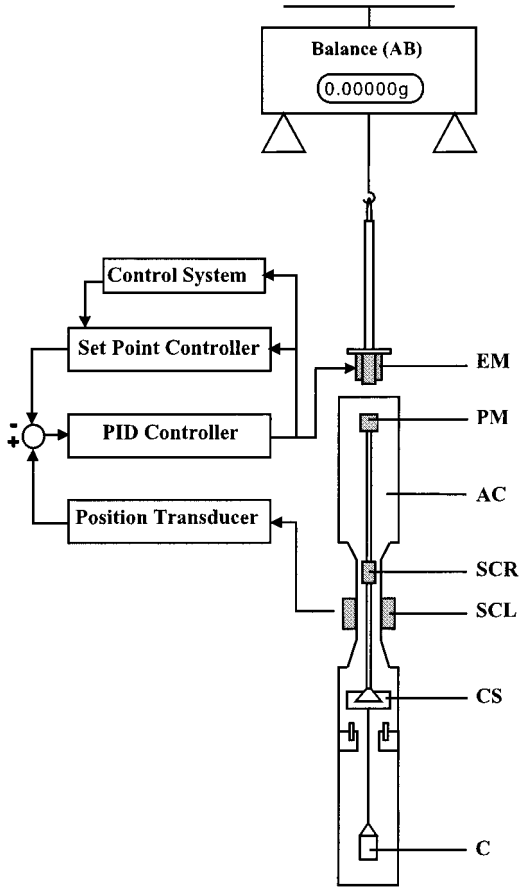

Figure 1. Principle of the magnetic suspension balance: (AB) analytical balance; (EM) electromagnet; (PM) permanent magnet; (AC) adsorption chamber; (SCR) sensor core; (SCL) sensor coil; (CS) coupling system; (C) crucible.

The pressure limit is set by the mechanical resistance of the adsorption chamber. The temperature limitation is set by the only electrical component still present in the incubator: the electrovalves.

Experimental Procedure. Prior to all operations, the sample is regenerated under vacuum (<1 Pa) at 423 K (local heating system) for 8 h using a diffusion pump. The regeneration procedure has been determined by a previous study of the regeneration parameters achieved on a thermobalance. Successive amounts of adsorbate are then admitted in the adsorption chamber. After each admission, the pressure, the temperature, and the adsorbed mass are measured at regular intervals. Once equilibrium is reached, the temperature, pressure, and mass signals are stored and a new amount of gas is admitted. The procedure is fully automated. The average time to obtain one adsorbed mass is 30 min, that is, a whole day for a 25-point isotherm. Details of the operating procedure are described in a previous publication.[12]

Measurement Precision. The analytical balance has a measurement precision of 0.01 mg. The relative error on the sample mass (≈2 g) is thus 0.001%. During the experiment, the equilibrium is considered to be reached on the mass point of view once four of the five last mass measurements (every 2-min measurements) differ by less than 0.02 mg. The maximum relative error on the adsorbed mass, observed for the lowest adsorbed mass we measured, is 0.1%.

The measurement precision of the pressure transducer ranges from 0.5 kPa (for the minimum working range: 0−0.5 MPa) to 10 kPa (for the maximum working range:

0−10 MPa). The maximum relative error on the lowest pressure we measured is 3%.

The temperature is measured with a precision of 0.1 K. The temperature stability limits the measurement uncertainty to 1 K.

These comments on the measurement precision do not take into account the error on the correction of the buoyancy effect.

Buoyancy Effect. Due to the variation of pressure, the buoyancy effect is not constant along the isotherm: It may become significant at high pressure. This effect can be divided into two contributions: The first one is due to the volume of the adsorbent + crucible system; its variation is due to the gas density change. The second one is due to the volume of the adsorbed phase; its variation is due to the gas density change on one hand and to the adsorbed phase volume change on the other hand.

The first contribution can be calculated by eq 1,

$$m_A = m_T - \rho^f(T,P)V_{ads+cruc} \quad (1)$$

in which m_A is the measured mass of the system (adsorbent + crucible + adsorbed phase), that is, the apparent mass, m_T is the real mass of the system if the second contribution is neglected, ρ^f is the density of the gas at temperature T and pressure P, and $V_{ads+cruc}$ is the volume of the system including the adsorbent and the crucible.

ρ^f is calculated as a function of temperature and pressure using a modified BWR equation of state. $V_{ads+cruc}$ is determined by a classical helium procedure. Helium can be considered as a nonadsorbable gas. Consequently, measuring the variation of m_A as a function of pressure leads to the determination of $V_{ads+cruc}$ by using eq 1 (the variation of m_T is then zero). Using this procedure, we have shown that helium is weakly adsorbed at low pressure. At pressure higher than 0.5 MPa the adsorbed mass is probably constant: we observed a linear variation of m_A with pressure. This behavior is due to the linear evolution of ρ^f with pressure and to the fact that the adsorption is completed at such high pressures. $V_{ads+cruc}$ is thus easily determined from the slope of m_A versus P. It is generally considered that using such a procedure, $V_{ads+cruc}$ is the volume of the system consisting of the crucible and the matrix of the adsorbent. This statement results from the assumption that the total pore volume is accessible to the gas phase. Given helium is considered to be nonadsorbed, such an assumption is coherent. Our experimental observations have shown that it was wrong. A part of the porosity of the adsorbent is included in $V_{ads+cruc}$.

The second contribution to the buoyancy effect could be calculated by

$$m_T = m - \rho^f(T,P)V_{ap} \quad (2)$$

in which m_T is the mass of the system (adsorbent + crucible + adsorbed phase) determined by eq 1, m is the real mass of the system taking into account both contributions of the buoyancy effect, and V_{ap} is the volume of the adsorbed phase.

V_{ap} is a function of the temperature and pressure. It increases with the micropore filling and with the multilayer formation in the meso- and macropores during the adsorption process. The evolution of V_{ap} cannot be accurately determined neither by experimental means nor by theoretical calculations. Considering the assumption we made on $V_{ads+cruc}$, V_{ap} ranges from 0 under vacuum to $m_{sample}\ V_p$ for a relative pressure equal to 1 (m_{sample} is the mass of the evacuated adsorbent and V_P is the total pore volume of the adsorbent given in Table 1).

Table 3. N_2 Excess Adsorbed Mass m^E on Activated Carbon F30/470 as a Function of Pressure at 303 K, 323 K and 343 K

T = 303 K		T = 323 K		T = 343 K	
P, kPa	m^E, kg kg^1	P, kPa	m^E, kg kg^{-1}	P, kPa	m^E, kg kg^{-1}
390	0.0229	630	0.0254	470	0.0151
640	0.0326	1160	0.0386	940	0.0259
830	0.0391	1670	0.0477	1370	0.0337
1020	0.0445	2240	0.0557	1780	0.0400
1580	0.0570	2740	0.0614	2180	0.0450
1800	0.0609	3260	0.0662	2560	0.0491
2240	0.0674	3780	0.0701	3020	0.0533
2600	0.0720	4240	0.0729	3440	0.0567
3020	0.0762	4730	0.0755	3830	0.0593
3800	0.0829	5290	0.0775	4200	0.0615
4220	0.0857	5780	0.0790	4650	0.0637
4610	0.0876	6230	0.0801	5060	0.0654
4990	0.0890	6690	0.0810	5450	0.0670
5350	0.0904	7190	0.0817	5800	0.0680
5710	0.0915	7620	0.0822	6210	0.0691
6050	0.0922	8060	0.0823	6600	0.0700
6470	0.0929	8530	0.0824	6990	0.0707
6980	0.0936	9020	0.0827	7350	0.0711
7410	0.0941	9470	0.0824	7690	0.0713
7800	0.0940			8050	0.0717
8160	0.0942			8420	0.0721
8470	0.0941			8760	0.0721
8780	0.0939			9100	0.0720
9140	0.0938			9470	0.0723
9500	0.0934				

Table 4. N_2 Excess Adsorbed Mass m^E on Activated Carbon F30/470 as a Function of Pressure at 363 K and 383 K

T = 363 K				T = 383 K			
P, kPa	m^E, kg kg^{-1}	P, kPa	m^E, kg kg^{-1}	P, kPa	m^E, kg kg^{-1}	P, kPa	m^E, kg kg^{-1}
480	0.0119	5270	0.0565	500	0.0100	4870	0.0472
790	0.0182	5650	0.0578	730	0.0139	5110	0.0481
1110	0.0235	6000	0.0587	970	0.0174	5530	0.0492
1410	0.0280	6330	0.0597	1180	0.0201	5910	0.0503
1710	0.0318	6640	0.0603	1550	0.0245	6280	0.0511
1990	0.0351	7060	0.0611	1900	0.0282	6620	0.0523
2490	0.0400	7410	0.0615	2240	0.0316	6920	0.0526
2920	0.0437	7690	0.0621	2570	0.0341	7490	0.0534
3390	0.0472	8250	0.0626	2880	0.0366	7910	0.0542
3940	0.0505	8810	0.0628	3350	0.0397	8430	0.0547
4420	0.0531	9200	0.0628	3900	0.0428	8930	0.0550
4870	0.0550	9470	0.0635	4410	0.0452	9460	0.0555

Now that the major technical problems relevant to high-temperature and high-pressure adsorption measurements have been outlined, the calculation of the buoyancy correction appears to be the last challenge to face in this particular domain. The first contribution has been calculated by eq 1 using the helium procedure to determine $V_{ads+cruc}$. This procedure is widespread and accepted. Few authors have dealt with the second contribution.[16−18] The correction of the second contribution as proposed by these authors requires theoretical developments. That is the reason high-pressure adsorption data are always presented as excess isotherms.

The excess adsorbed mass is defined by

$$m^E = \frac{m_T - (m_{sample} + m_{crucible})}{m_{sample}} \quad (3)$$

in which $m_{crucible}$ is the mass of the crucible.

Although we did our own proposals for the calculation of the second contribution of the buoyancy effect,[18,19] we

Table 5. CH_4 Excess Adsorbed Mass m^E on Activated Carbon F30/470 as a Function of Pressure at 303 K, 323 K, and 343 K

T = 303 K		T = 323 K		T = 343 K	
P, kPa	m^E, kg kg^{-1}	P, kPa	m^E, kg kg^{-1}	P, kPa	m^E, kg kg^{-1}
540	0.0384	440	0.0266	530	0.0244
810	0.0472	860	0.0395	750	0.0300
1080	0.0537	1270	0.0478	960	0.0345
1360	0.0589	1570	0.0524	1160	0.0381
1600	0.0627	1800	0.0553	1370	0.0414
1820	0.0654	2020	0.0578	1770	0.0465
2220	0.0696	2440	0.0616	2120	0.0501
2550	0.0723	2850	0.0646	2470	0.0530
3100	0.0758	3210	0.0666	2810	0.0554
3630	0.0783	3700	0.0689	3140	0.0575
4170	0.0803	4130	0.0706	3440	0.0589
4640	0.0811	4650	0.0721	3990	0.0613
5030	0.0819	5040	0.0729	4480	0.0627
5370	0.0822	5410	0.0734	4930	0.0639
5710	0.0827	5770	0.0739	5330	0.0646
6140	0.0826	6070	0.0740	5680	0.0651
6550	0.0825	6370	0.0741	6000	0.0653
6920	0.0824	6670	0.0744	6290	0.0653
7270	0.0823	7170	0.0743	6620	0.0658
7590	0.0820	7490	0.0742	7120	0.0658
7870	0.0817	7780	0.0740	7470	0.0652
8170	0.0812	8030	0.0737	7750	0.0653
8460	0.0809	8530	0.0733	8020	0.0647
8970	0.0799	8980	0.0726	8490	0.0640
				8980	0.0625

Table 6. CH_4 Excess Adsorbed Mass m^E on Activated Carbon F30/470 as a Function of Pressure at 363 K and 383 K

T = 362 K				T = 383 K			
P, kPa	m^E, kg kg^{-1}	P, kPa	m^E, kg kg^{-1}	P, kPa	m^E, kg kg^{-1}	P, kPa	m^E, kg kg^{-1}
290	0.0124	5160	0.0568	340	0.0105	4930	0.0491
510	0.0189	5580	0.0577	590	0.0162	5370	0.0499
730	0.0240	5950	0.0580	900	0.0217	5770	0.0508
950	0.0281	6270	0.0581	1200	0.0261	6190	0.0512
1170	0.0316	6660	0.0586	1500	0.0297	6700	0.0519
1400	0.0349	7050	0.0586	1790	0.0327	7040	0.0520
1810	0.0394	7400	0.0584	2090	0.0354	7380	0.0523
2220	0.0433	7730	0.0581	2380	0.0377	7690	0.0523
2590	0.0462	8090	0.0577	2920	0.0413	8060	0.0522
2930	0.0485	8530	0.0572	3460	0.0440	8420	0.0523
3270	0.0502	8900	0.0568	4010	0.0464	8820	0.0523
3890	0.0530	9160	0.0558	4490	0.0477	9240	0.0519
4440	0.0549						

do not apply these correction calculations to the data we present in this paper. Consequently, our data are also excess adsorption isotherms. This is understandable as the exactness of experimental results should not depend on any theoretical model. However, one must be careful when using such excess data. It is necessary to have an idea of the error due to the second contribution of the buoyancy effect.

Experimental Results

Tables 3−8 present the experimental excess adsorbed mass as a function of pressure at temperatures of 303 K, 323 K, 343 K, 363 K, and 383 K for N_2, CH_4, and C_3H_8 on activated carbon F30/470. The isotherms are presented in Figures 2−4. Figure 5 shows a comparison between the N_2 adsorption data at 303 K obtained by two different methods: the gravimetric method presented in this paper and a volumetric method presented elsewhere.[10] The maximum working pressure of this last method is 4 MPa. The average deviation between these two sets of results is <3.5%.

Table 7. C_3H_8 Excess Adsorbed Mass m^E on Activated Carbon F30/470 as a Function of Pressure at 303 K, 323 K, and 343 K

T = 303 K		T = 323 K		T = 343 K	
P, kPa	m^E, kg kg^{-1}	P, kPa	m^E, kg kg^{-1}	P, kPa	m^E, kg kg^{-1}
50	0.1771	67	0.1570	105	0.1525
91	0.1933	152	0.1826	216	0.1750
181	0.2105	226	0.1939	318	0.1861
265	0.2196	304	0.2017	434	0.1944
349	0.2261	381	0.2072	547	0.2002
469	0.2331	458	0.2116	657	0.2045
573	0.2384	603	0.2178	764	0.2079
694	0.2441	736	0.2223	862	0.2105
782	0.2486	852	0.2256	956	0.2126
886	0.2552	956	0.2282	1042	0.2142
976	0.2655	1086	0.2313	1203	0.2169
		1188	0.2337	1344	0.2187
		1294	0.2363	1467	0.2200
		1393	0.2391	1574	0.2211
		1462	0.2418	1686	0.2219
				1809	0.2230
				1893	0.2234
				2024	0.2242
				2201	0.2257

Table 8. C_3H_8 Excess Adsorbed Mass m^E on Activated Carbon F30/470 as a Function of Pressure at 363 K and 383 K

T = 363 K				T = 383 K			
P, kPa	m^E, kg kg^{-1}	P, kPa	m^E, kg kg^{-1}	P, kPa	m^E, kg kg^{-1}	P, kPa	m^E, kg kg^{-1}
214	0.1549	1927	0.2032	206	0.1329	2767	0.1850
400	0.1733	2010	0.2038	466	0.1578	2843	0.1842
586	0.1832	2124	0.2039	719	0.1696	2922	0.1836
769	0.1896	2224	0.2037	871	0.1745	3060	0.1820
925	0.1933	2307	0.2031	1024	0.1780	3182	0.1810
1088	0.1965	2506	0.2018	1192	0.1809	3291	0.1797
1235	0.1987	2679	0.2003	1332	0.1828	3389	0.1781
1374	0.2002	2835	0.1988	1491	0.1845	3560	0.1758
1502	0.2011	2985	0.1963	1640	0.1855	3719	0.1714
1624	0.2020	3091	0.1931	1766	0.1861	3868	0.1667
1735	0.2026	3228	0.1904	1903	0.1865	3948	0.1648
1833	0.2028			2056	0.1870	4113	0.1570
				2162	0.1869	4222	0.1488
				2297	0.1869	4299	0.1429
				2406	0.1866	4378	0.1330
				2501	0.1864	4466	0.1231
				2602	0.1859		
				2687	0.1857		

Results and Comments

Both N_2 and CH_4 excess isotherms exhibit similar behaviors, a progressive mass uptake with increasing pressure. At high pressure, the slope of the isotherms decreases and is nearly equal to zero at the end of the isotherms. The slope of the CH_4 isotherms and of the 303 K and 323 K N_2 isotherms are negative at very high pressure (near 10 MPa). Such a behavior is due to the fact that we are considering excess adsorption isotherms. At high pressure, the gas density is high so that the term $\rho^f(T,P)V_{ap}$ in eq 2 is large. Besides, the mass uptake is low (constant adsorbed mass at high pressure): m does not increase anymore. Consequently, the excess mass m^E (as defined in eq 3) decreases. The C_3H_8 excess isotherms exhibit high initial slopes corresponding to the high adsorption energies in the micropores. C_3H_8 has a high affinity for the graphite surface (adsorption energy of C_3H_8 on graphite is 25038 J mol^{-1}) and the porous structure of the activated carbon is responsible for the adsorption energy enhancement. The Henry's constant is high and the micropore filling is completed at quite low pressure. The

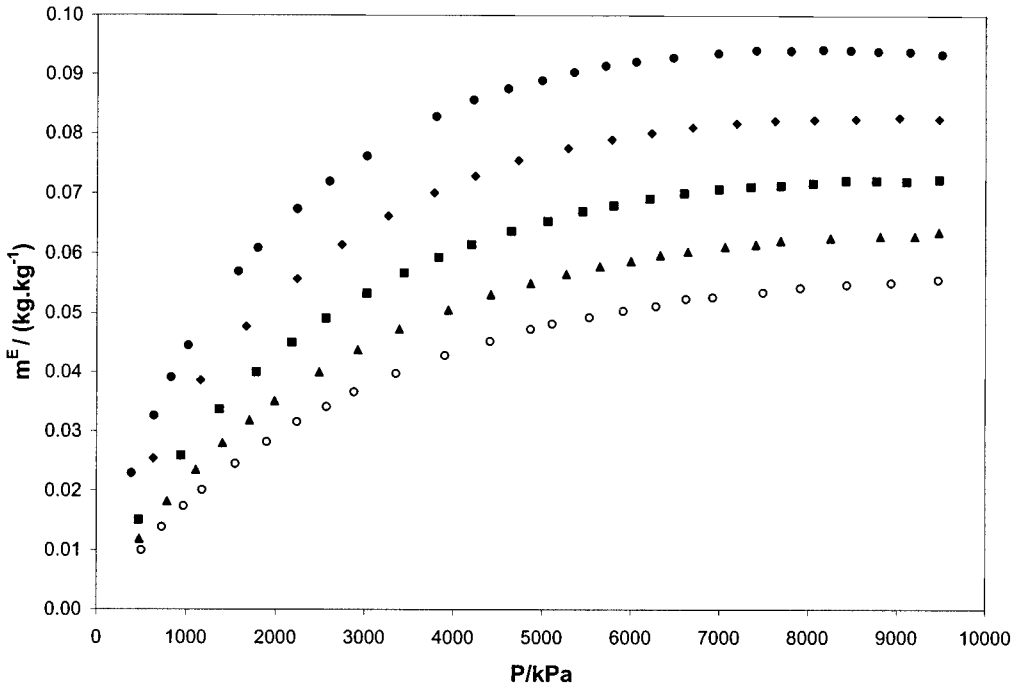

Figure 2. Excess adsorption isotherms of N_2 on activated carbon F30/470: (●) 303 K; (◆) 323 K; (■) 343 K; (▲) 363 K; (○) 383 K.

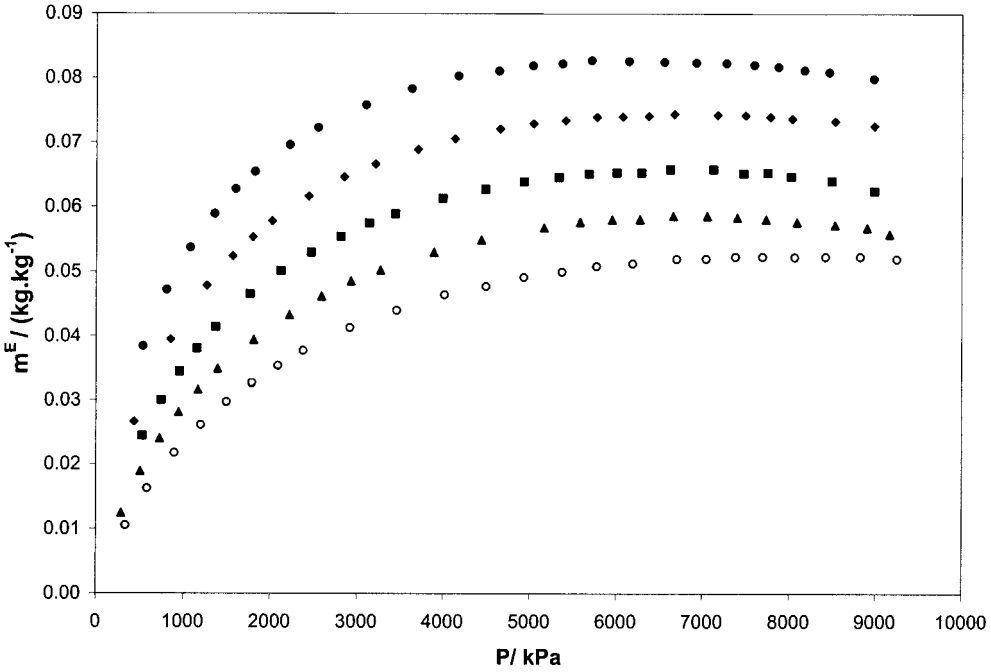

Figure 3. Excess adsorption isotherms of CH_4 on activated carbon F30/470: (●) 303 K; (◆) 323 K; (■) 343 K; (▲) 363 K; (○) 383 K.

low-temperature C_3H_8 isotherms (303 K, 323 K, and 343 K) exhibit a low slope at medium pressure (multilayer adsorption in the mesopores) and another steeper increase near the saturation pressure (capillary condensation.). The high-temperature C_3H_8 isotherms exhibit a negative slope at high pressure. This is particularly true for the 383 K isotherm (supercritical isotherm). The explanation for such a behavior is the same as the one given for the CH_4 and N_2 isotherms. These results show that the influence of the second contribution of the buoyancy effect is easily observable for supercritical fluids. Considering the 363 K C_3H_8 isotherm, it must be noticed that the results near the saturation pressure are not presented because they are not reliable. Indeed, the critical temperature of C_3H_8 is 369.8 K so that at 363 K we approach the critical conditions for pressure larger than 3.5 MPa. Consequently, the error on ρ^f in eq 1 does not allow a correct calculation of the first contribution of the buoyancy effect. A simultaneous experimental determination of the gas density and of the adsorbed mass would help to correct the unefficiency of the calculation of the buoyancy effect correction in such particular conditions.

It should be noticed that the fact that the isotherms do not exhibit any negative slope area does not mean that the influence of the buoyancy effect on the adsorbed phase (second contribution of the buoyancy effect) can be neglected. It is not the purpose of this paper to present a complete study of this buoyancy effect on the adsorbed phase. It has no effect on the validity of the excess data we provide in this paper.

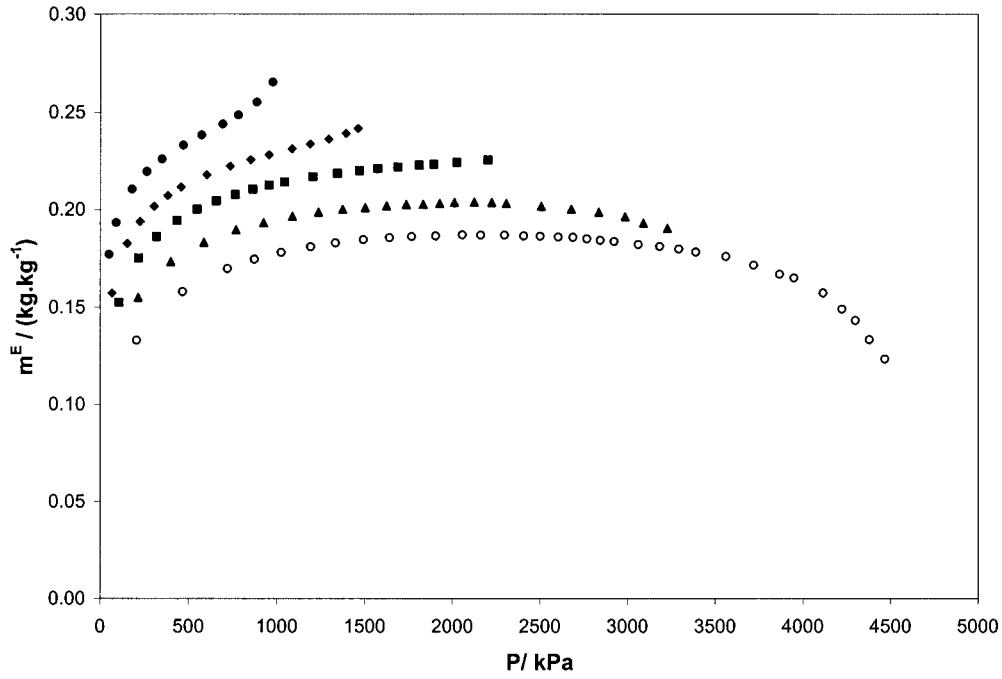

Figure 4. Excess adsorption isotherms of C_3H_8 on activated carbon F30/470: (●) 303 K; (◆) 323 K; (■) 343 K; (▲) 363 K; (○) 383 K.

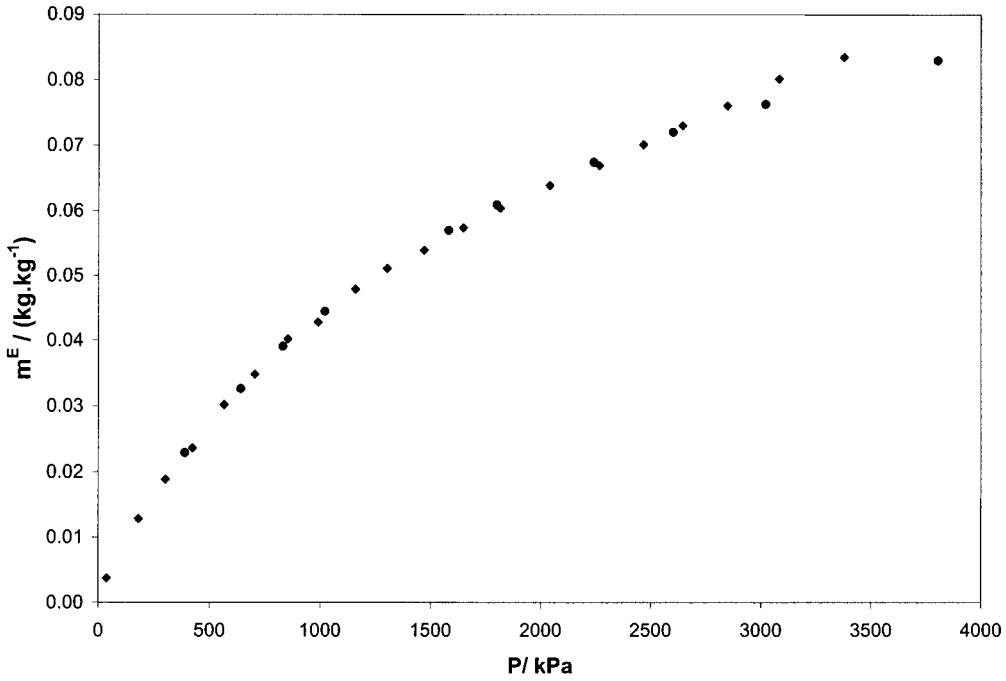

Figure 5. Comparison of the gravimetric and volumetric methods based on the 303 K N_2 adsorption isotherms: (●) gravimetric method; (◆) volumetric method.

Conclusions

In this paper we present excess adsorption isotherms for N_2, CH_4, and C_3H_8 on an activated carbon (F30/470 Chemviron Carbon) for pressures ranging from 0 to 10 MPa (when not limited by the vapor pressure of the adsorbate) and for temperatures ranging from 303 K to 383 K. These measurements have been obtained using a special experimental device which makes possible the data acquisition for adsorbates which could condense in the cold spots of classical apparatuses in such simultaneous high-temperature and high-pressure conditions. This particular advantage was useful for the determination of the C_3H_8 data. The experimental excess adsorption isotherms we obtained show the striking influence of the buoyancy effect on the adsorbed phase for supercritical gases. Some comments and references about the correction of this disturbing effect are provided.

Literature Cited

(1) Matranga, K. R.; Myers, A.-L.; Glandt, E. D. Storage of Natural Gas by Adsorption on Activated Carbon. *Chem. Eng. Sci.* **1992**, *47*, 1569−1579.

(2) Talu, O. An Overview of Adsorption Storage of Natural Gas. In *Proceedings of the IVth Conference on Fundamentals of Adsorption*; Elsevier: Amsterdam, 1993; pp 655−662.

(3) Mota, J. P. B.; Rodrigues, A. E.; Saatdjan, E.; Tondeur, D. Charge Dynamics of a Methane Adsorption Storage System: Intraparticle Diffusional Effects. *Adsorption* **1997**, *3*, 117−125.

(4) Mota, J. P. B. A Theoretical Study of the Impact of Heavy Impurities on the Performances of Natural Gas Adsorptive

Storage Systems. In *Proceedings of the VIth Conference on Fundamentals of Adsorption*; Elsevier: Paris, 1998; pp 1095−1100.
(5) Szarzynski, S.; Pons, M. A Novel Experimental Unit for Adsorptive Refrigeration with Heat Regeneration. In *Proceedings of the VIth Conference on Fundamentals of Adsorption*; Elsevier: Paris, 1998; pp 113−118.
(6) Critoph, R. E.; Tamainot-telto, Z.; Davies, G. N. L. Adsorption Refrigerator using a Monolithic Carbon−Aluminium Laminate Adsorbent and Ammonia Refrigerant. In *Proceedings of the 1999 sorption heat pump conference*; Bayerisches Zentrum für Angewandte Energie Forschung E. V.: Munich, 1999; pp 349−353.
(7) Vasiliev, L. L.; Mishkinis, D. A.; Antuh, A. A.; Vasiliev, L. L., Jr. Solar Gas−Solid Sorption Heat Pump. In *Proceedings of the 1999 sorption heat pump conference*; Bayerisches Zentrum für Angewandte Energie Forschung E. V.: Munich, 1999; pp 117−122.
(8) Specovius, J.; Findenegg, G. H. Physical Adsorption of Gases at High Pressure: Argon and Methane on Graphitized Carbon Black. *Ber. Bunsen-Ges. Phys. Chem.* **1978**, *82*, 174−180.
(9) Vidal, D.; Malbrunot, P.; Guengant, L.; Vermesse, J.; Bose, T. K.; Chahine, R Measurement of Physical Adsorption of Gases at High Pressure *Rev. Sci. Instrum.* **1990**, *61* (4), 1314−1318.
(10) Berlier, K.; Bougard, J.; Olivier, M.-G. Automated Measurement of Isotherms of Adsorption on Microporous Media in Large Ranges of Pressure and Temperature. *Meas. Sci. Technol.* **1995**, *6*, 107−113.
(11) Frère, M.; De Weireld, G.; Jadot, R. Adsorption Isotherms Measurements at High Pressure and High Temperature. In *Proceedings of the VIth Conference on Fundamentals of Adsorption*; Elsevier: Paris, 1998; pp 279−284.
(12) De Weireld, G.; Frère, M.; Jadot, R. Automated Determination of High Temperature and High-Pressure Adsorption Isotherms Using a Magnetic Suspension Balance. *Meas. Sci. Technol.* **1999**, *10*, 117−126.
(13) Berlier, K.; Frère, M. Adsorption of CO_2 on Microporous Materials *J. Chem. Eng. Data* **1997**, *42* (3), 533−537.
(14) Frère, M.; Berlier, K.; Bougard, J.; Jadot, R. Adsorption of Dichlorodifluoromethane, Chlorodifluoromethane, Chloropentafluoroethane, 1−1 Difluoroethane and 1−1−1−2 Tetrafluoroethane on Silica Gel. *J. Chem. Eng. Data* **1994**, *39* (4), 697−699.
(15) Stewart, R. B.; Jacobsen, R. T.; Penoncello, S. G. *Thermodynamics Properties of Refrigerants*; American Society of Heating, Refrigerating and Air Conditioning Engineers Inc.: Atlanta, 1986.
(16) Staudt, R.; Saller, G.; Tomalla, M.; Keller, J. U. A note on Gravimetric Measurement of Gas Adsorption Equilibria. *Ber. Bunsen-Ges. Phys. Chem.* **1993**, *97* (1), 98−105.
(17) Neimark, A. V.; Ravikovitch, P. I. Calibration of Adsorption Theories. In *Proceedings of the VIth Conference on Fundamentals of Adsorption*; Elsevier: Paris, 1998; pp 159−164.
(18) De Weireld, G.; Frère, M.; Jadot, R. Characterization of Porous Carbonaceous Sorbents using High Pressure−High-Temperature Adsorption Data. In *Proceedings of the 5th International Conference on Characterization of Porous Solids*; Elsevier Science B.V: Amsterdam, 2000; pp 333−345.
(19) Frère, M.; De Weireld, G. Study of the buoyancy effect on high pressure and high-temperature adsorption isotherms measurements. In *Proceedings of the VIIth International Conference on Fudamentals of Adsorption,* Nagasaki, May 2001; in press.

Received for review September 24, 2001. Accepted March 18, 2002.

JE010257S